공학석사 학위논문

Effect of LiF additive on combustion synthesis of $MgAl_2O_4$

$MgAl_2O_4$의 연소합성 중 LiF 첨가물의 영향

2017년 8월

서울대학교 대학원

재료공학부

Jin Jian

Effect of LiF additive on combustion synthesis of $MgAl_2O_4$

$MgAl_2O_4$의 연소합성 중 LiF 첨가물의 영향

지도 교수 강 신 후

이 논문을 공학석사 학위논문으로 제출함

2017년 7월

서울대학교 대학원

재료공학부

Jin Jian

Jin Jian의 공학석사 학위논문을 인준함

2017년 6월

위 원 장 ____박 찬____ (인)

부위원장 ____홍 성 현____ (인)

위 원 ____강 신 후____ (인)

Abstract

Due to the excellent mechanical properties and high transparency from near-UV to mid-IR ($190<\lambda<6000$nm), $MgAl_2O_4$ has been used for optical engineering applications, such as armored window systems, high energy laser windows and lightweight armor.

In order to fabricate high quality transparent ceramics, high quality starting powder is necessary.

So we focused on the combustion synthesis method which has recently drawn the attention of researchers due to multiply advantages. But the combustion synthesis method still have some disadvantages need to be overcome. Based on the mechanism of spinel formation, we decided to introduce some additive to improve this method. After calculation, the promising of LiF additive was certified.

With different amount of LiF, combustion synthesis of $MgAl_2O_4$ (MAS) was investigated in relation to the synthesis conditions, powder properties, thermodynamic aspects and sinterability. Using citric acid as a single fuel, only hard-agglomeration MAS was obtained with high carbon contamination and poor sinterability which cannot be used as transparent ceramic raw materials. However, by introducing LiF, good property MAS powder can be synthesized. This is because LiF can effectively reduce the formation energy of MAS, remove the residue carbon, reduce agglomeration degree and promote the crystal growth during the combustion reaction. Through 2-steps calcination, the as-obtain high purity powders have been consolidated into transparent ceramics (T=81.0%) by SPS at T=1200℃ for 20min holding under P=80MPa

Key word: $MgAl_2O_4$, Nanocrystals, Combustion synthesis, LiF, transparency

Student Number: 2015-22306

Table of Contents

List of Figures

List of Tables

Chapter 1. Introduction

1.1. Study Background

Recent years, with the increasing demand for high-performance materials, ceramic materials re-appeared in the public view. Various kinds of ceramics have been researched, such as transparent ceramic materials. Transparent polycrystalline ceramics are a new development that has engendered considerable interest for optical applications that only few materials can satisfy.[4]

As one of the transparent polycrystalline ceramics, magnesium aluminum spinel ($MgAl_2O_4$) possesses high optical transmission in the ultraviolet, visible, and infrared spectral ranges(**Fig.1-1**) and excellent mechanical properties[5], which has become well-known optical materials for both industrial and military applications (e.g., high-pressure arc lamps, optical heat exchangers, transparent armor, missile domes, etc.)[3]. (**Fig.1-2**)

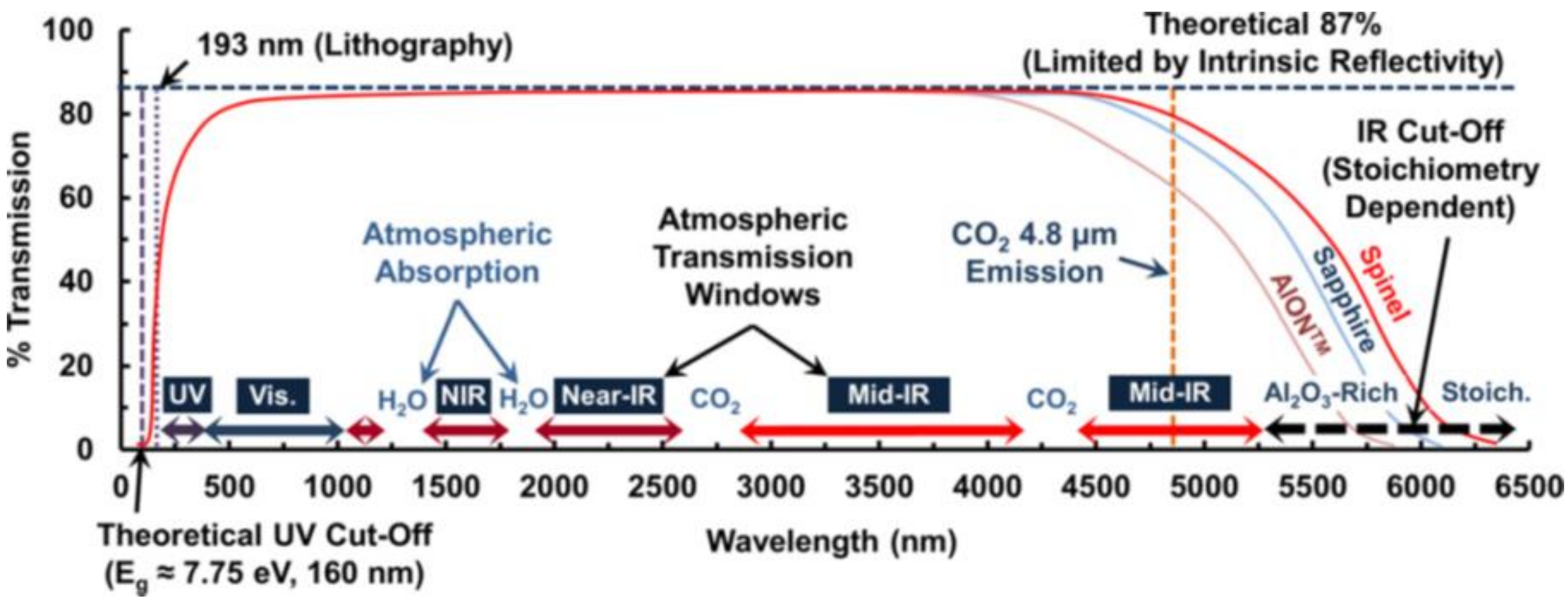

Fig.1-1 Typical transmission spectrum for transparent polycrystalline spinel.[2, 3]

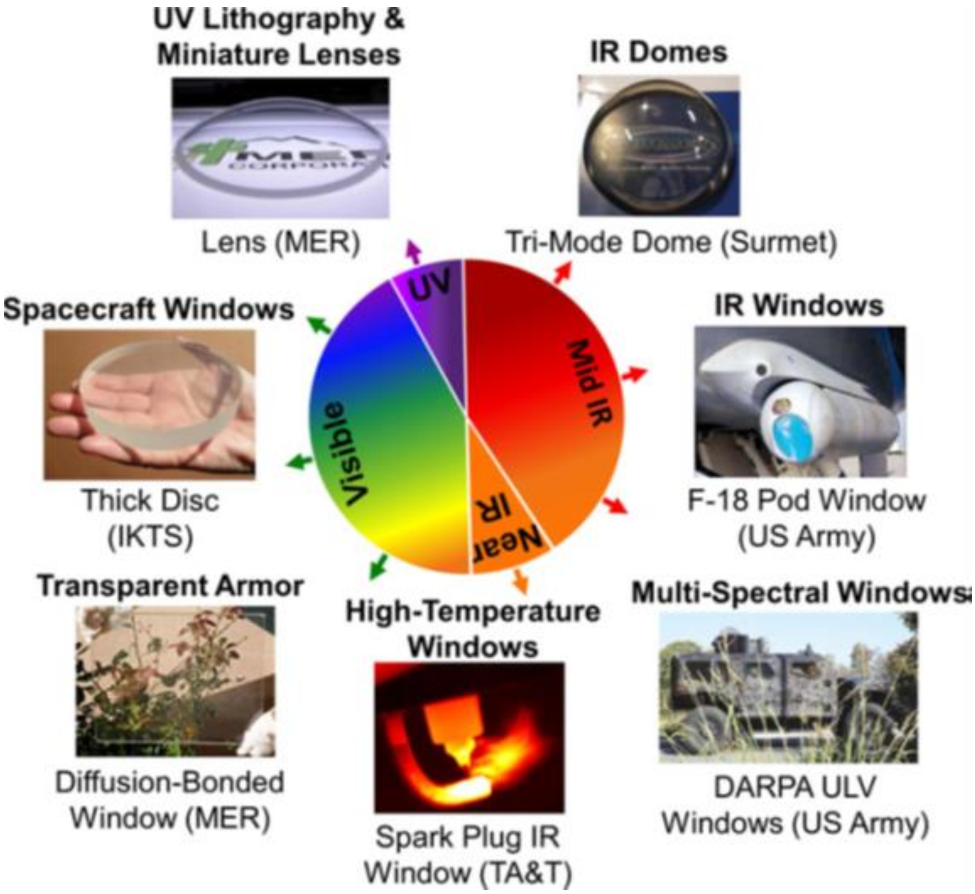

Fig. 1-2 Select applications and transparent spinel components, reproduced with permission.[3]

1.2. Synthesis of $MgAl_2O_4$ Powders

To fabricate high quality transparent windows, utmost care should be taken throughout the process from the synthesis of high quality starting powder.

Fig.1-3 shows the procedures of solution-based methods: sol-gel, co-precipitation, hydrothermal, and combustion methods, respectively.[1] We focused on the combustion synthesis method which has recently drawn the attention of researcher due to the multiple advantages such as mass production, high purity and high homogeneity. (**Table 1-1**)

For combustion synthesis method, an exothermic and oxidative reaction will occurs at low temperature leading to a sudden temperature of more than 1200℃ within a short time, resulting in a powder as final product.

Because of this short time of reaction, nanocrystalline powders are produced, but it is combined with some disadvantages such as hard agglomeration, excessive residual carbon content and low sinerability. So we improved this synthesis method by introducing the additives-LiF.

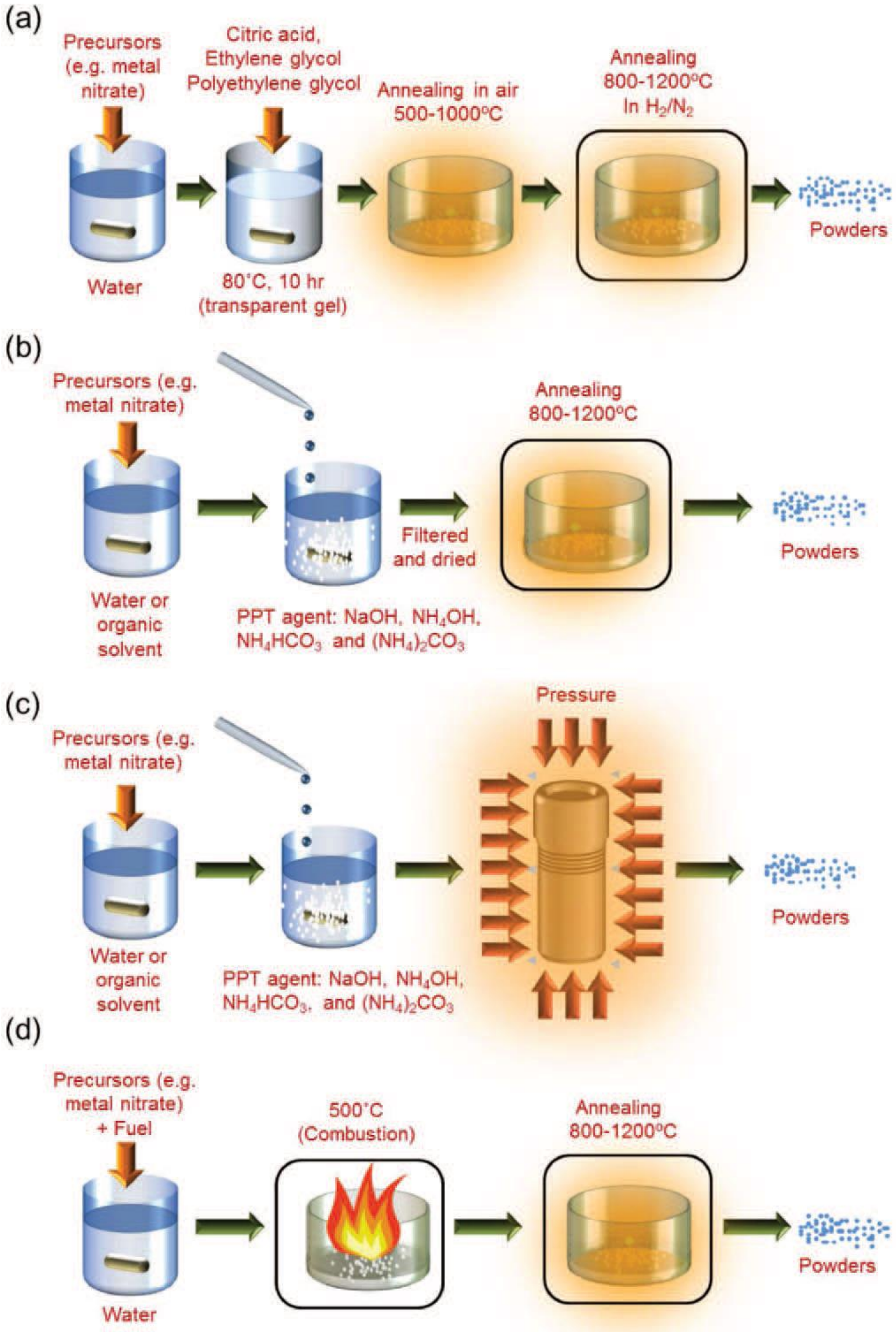

Fig. 1-3 Schematic diagram of solution based synthesismethods: (a) sol-gel, (b) co-precipitation, (c) hydrothermal, and (d) combustion.

Synthesis method	Sol-Gel	Co-Precipitation	Hydrothermal	Combustion
Particle Size	10 nm – 2 um	10 nm – 1 um	10 nm – 1 um	500 nm – 2 um
Size Distribution	Narrow	Narrow	Narrow	Medium
Morphological Control	Medium	Very Good	Good	Poor
Purity	Good	Medium	Medium – Good	Medium – Good
Cost	Medium	Medium	Medium – High	**Low – Medium**
Synthesis time	Medium	Medium	Very Long	**Short**
Limitation	Soluble Precursor Carbon Contamination	Soluble Precursor	No mass production Special Equipment	Hard Agglomeration Carbon Contamination

Table 1-1. Summary of synthesis methods: particle size, morphology control, purity, cost, time and limitations.[1]

1.3. LiF Additive

1.3.1. Sintering Additive

As a commonly used sintering additive, LiF melts at ~850℃, wets spinel, [6] spreads over surfaces by capillarity,[6] and likely aids densification by particle rearrangement and liquid-phase sintering.[3, 7] In addition to forming a transient liquid phase, LiF leads to the formation of oxygen vacancies that promote late-stage sintering in $MgAl_2O_4$.[7] (**Fig.1-4**)

1.3.2. Synthesis additive

LiF also can be used as the synthesis additive.

In a study, Balabanov, S.S. et al. [5] synthesized $MgAl_2O_4$ nanopowders by hydrolysis of magnesium aluminum double isopropoxide $MgAl_2(OPr^i)_8$ followed by the low-temperature calcination.(**Fig.1-5**) It has been determined that lithium fluoride sintering aid significantly enhances the crystallinity of spinel particles and facilitates obtaining of highly-faceted spinel grains. The average particle size increases from 30 nm for undoped spinel to 700–1000 nm for LiF-doped $MgAl_2O_4$ particles calcined at the same temperature of 900℃ due to formation of transient liquid phase during calcination of doped powders.

Huan Jiao et al.[8] synthesized YAG: Ce phosphors by LiF assisted sol-gel combustion method. YAG phase formed at 540℃ and without the intermediate phase appeared.(**Fig.1-6**) This was almost the lowest temperature to synthesis YAG phase without appearance of any impurities. It also reported that using of LiF can decrease the sintering temperature about 100-200℃.

Kostic et al.[9] studied the influence of fluorine ion (using AlF_3 or CaF_2) on the solid-state reaction synthesis of $MgAl_2O_4$. According to the similar ionic radii values between F ion and O^{2-} ion, F ion could be incorporated in the anion sublattice, increases the cation vacancy concentration, which intensifies the cation diffusion and completes spinel formation at a much lower temperature.

In this connection, the use of LiF as a synthesis additive for obtaining high quality $MgAl_2O_4$ nanopowder by combustion method is promising.

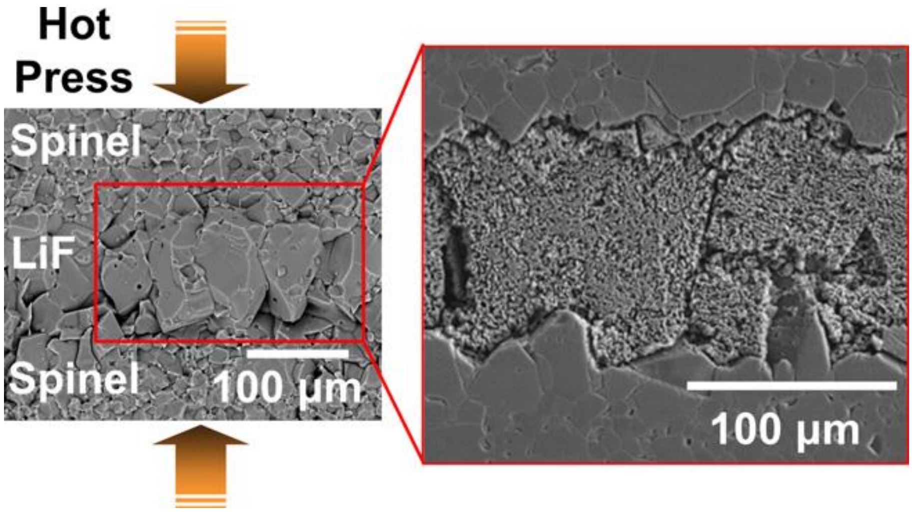

Fig. 1-4 Hot-pressed spinel/LiF/spinel sandwich structure and highly defected grains revealed by etching.[3]

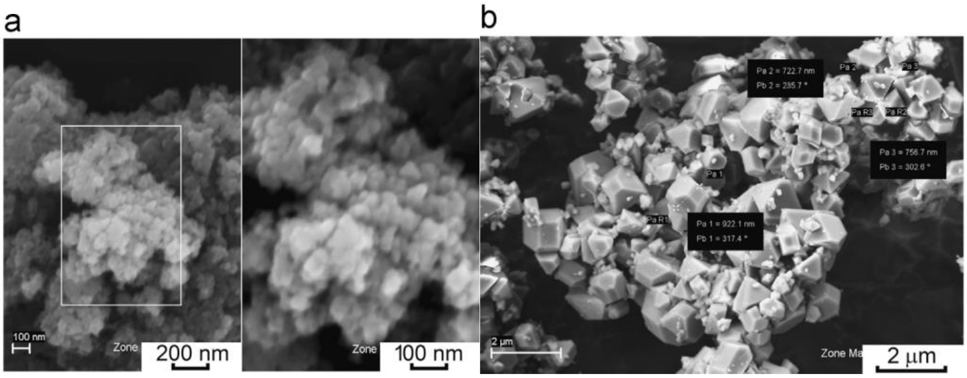

Fig. 1-5 SEM micrographs of $MgAl_2O_4$ (a) and $MgAl_2O_4$: LiF 3wt% powders (b) calcined at 900°C for 2h

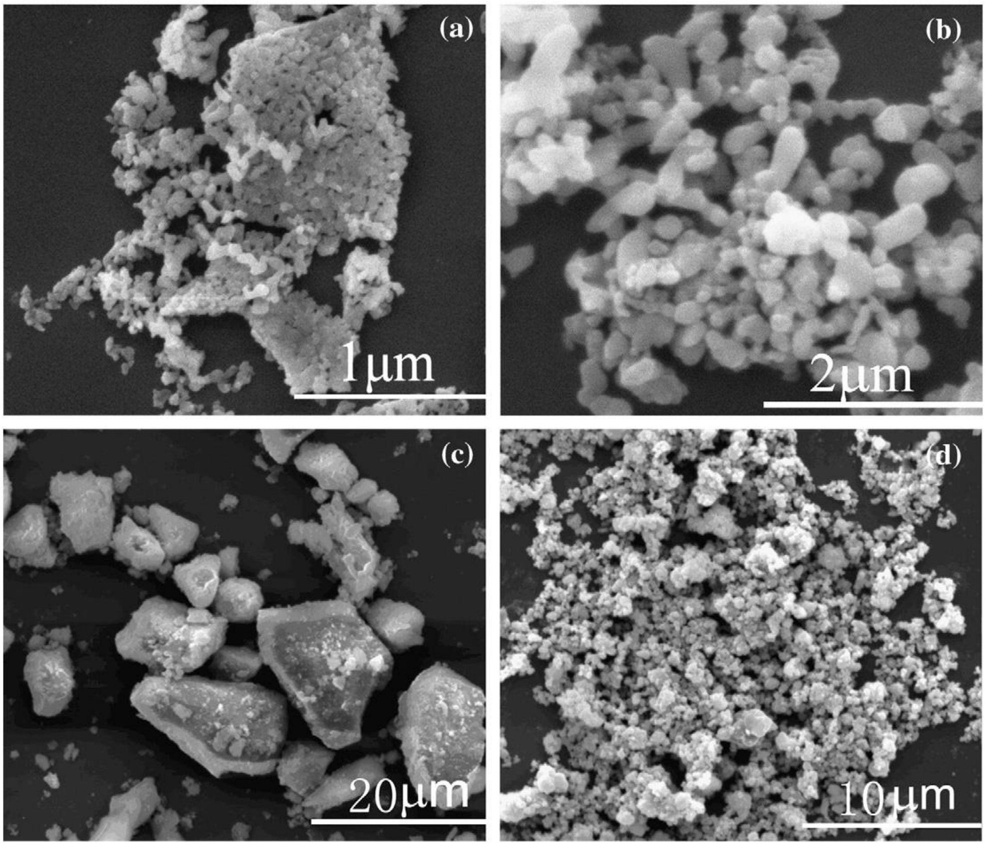

Fig. 1-6 SEM photograph of the as-prepared YAG: Ce powders calcined at 540 and 700°C with and without flux.

(a) Calcined at 540°C with flux; (b) Calcined at 700°C with flux;

(c) Calcined at 540°C without flux; (d) Calcined at 700°C without flux.

1.4. Objective of the Study

The objective of this dissertation is to improve the combustion synthesis method, through

1. the reduction of powder agglomeration
2. the reduction of residual carbon content
3. the optimization of particle size

through the aid of LiF, so as to mass produce the high quality $MgAl_2O_4$ powder, and fabricate the high transparency spinel in low sintering temperature.

Chapter 2. Experimental Methods

2.1. Sample Preparation

Magnesium nitrate hexahydrate ($Mg(NO_3)_2 \cdot 6H_2O$ -- sigma-aldrich), Aluminum nitrate nonahydrate ($Al(NO_3)_3 \cdot 9H_2O$ -- sigma-aldrich), Citric acid ($C_6H_8O_7$ -- sigma-aldrich), Ammonium hydroxide solution ($NH_3 \cdot H_2O$ -- sigma-aldrich), Lithium Fluoride (LiF -- sigma-aldrich) were used as raw materials for the preparation of $MgAl_2O_4$ powder. The experiment was designed to produce 0.008mol $MgAl_2O_4$. Based on Jain's rule, stoichiometric amount of magnesium nitrate, aluminum nitrate and fuel (citric acid) were mixed in 50ml deionized water, in order to obtain CO_2, H_2O and N_2 as reaction by-products. The pH of the solution was controlled to 7 by dropping ammonia solution under magnetic stirring. After the addition of an appropriate amount of LiF in the solution, the mixture was continue stirring at 120℃. After evaporation, the resulting gel was taken as a precursor. The precursors were calcined at 800/900/1000℃ for 1h, respectively, under air condition in order to obtain $MgAl_2O_4$.

The washing treatment was carried out to the as-calcined powders by Hydrochloric acid solution (HCl – Samchun). The washed powders were filtered using vacuum filtration with distilled water and dried in a freeze dryer for 20hr.

The powder which synthesized at 800℃ was divided into two categories after washing treatment, one without any treatment and the other one did the calcination at 1000℃ for 1h. And then did the sintering, respectively.

Sintering methods:

Air sintering: The powders were pressed by Cold Isostatic Pressing (CIP) at 200MPa and sintered at 1550℃ for 2hr in air condition with heating rate of 10min/℃.

SPS sintering: The sintering was conducted in a SPS apparatus (SPS-1050, Sumitomo). The powder was placed in a graphite die with a 10mm inner diameter, in which the powder and the die were separated by carbon sheets.[10] Under vacuum (10^{-3} torr) conditions, the sintering schedule as shown below. In order to optimize the sintering parameters, the sintering temperature was varied from 1150℃ – 1300℃.

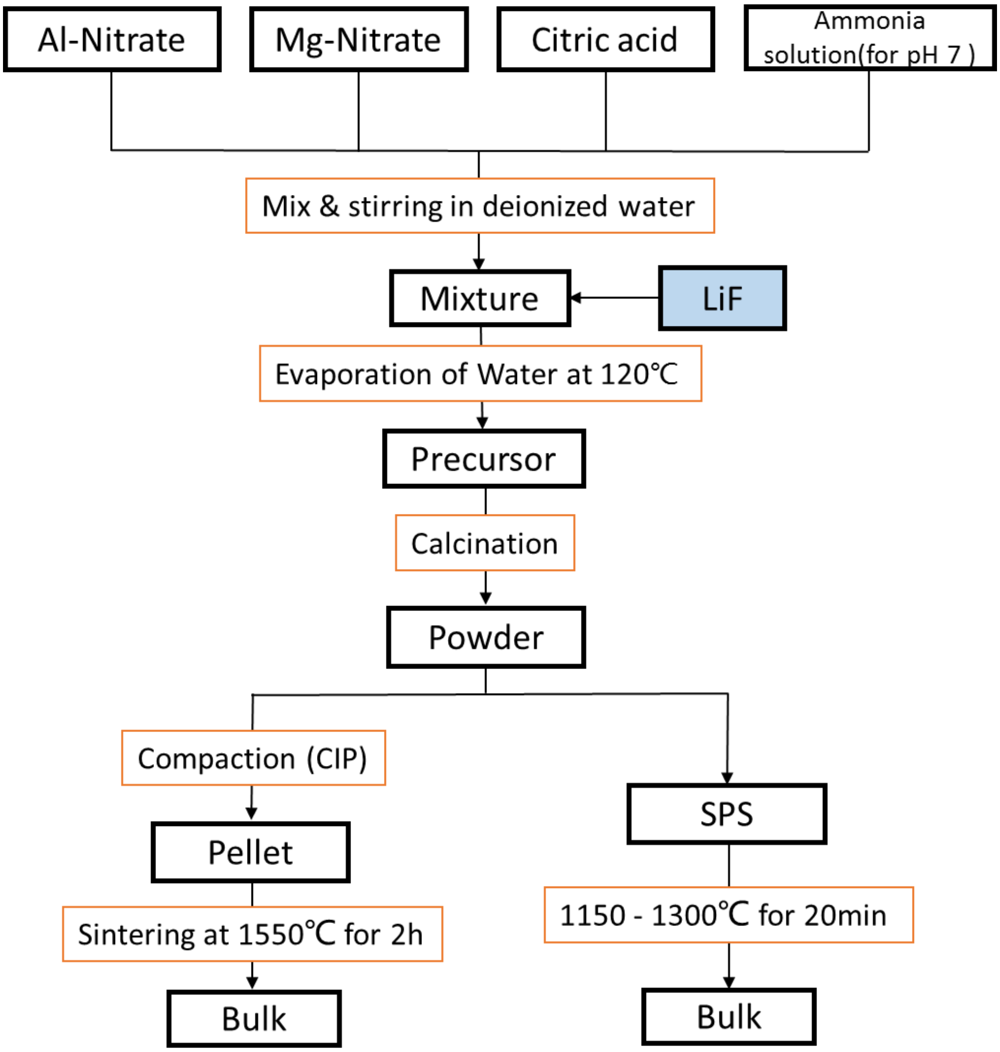

Fig. 2-1 experimental schedule

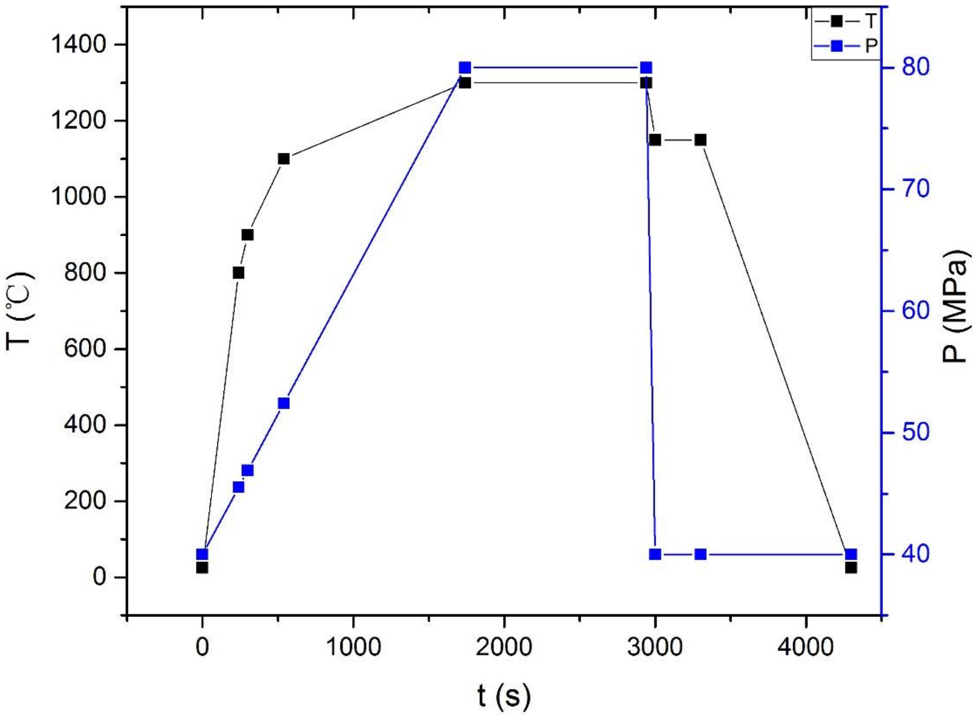

Fig. 2-2 SPS sintering schedule

2.2. Characterization Methods

Crystal structure of $MgAl_2O_4$ measurement was performed on Laboratory X-ray powder diffraction (XRD) with mono-chromatized CuKα radiation equipped with Vantec-1 linear detector. Data was collected between 10 ° and 80° (2θ) at room temperature with a 0.0164° step size. The calculation of crystallite sizes were performed based on Scherrer's method.

TGA-DSC analyses of precursor were carried out by Simultaneous DTA/TGA analyser at a heating rate of 10°C/min under a continuous air flow (50ml/min), in Pt crucibles.

The residual carbon content was measured by the Elemental (C, N, S) Analyzer (Flash EA 1112).

The morphology and size of powder samples were collected using Field Emission Scanning Electron Microscopy (FE-SEM) data collected on MERLIN Compact. The powder samples were placed on a carbon tape.

High Resolution Transmission Electron Microscopy (HRTEM) data was collected on a JEM-2100F type microscope. The powder samples were dispersed in actone and mixed by ultra-sonication, and few drops of the solution with the small crystallites in suspension was deposited onto carbon-coated copper grid.

Optical transmission spectra were recorded using a Cary 5000 UV-Vis-NIR spectrophotometer in the 0.35–1.6μm wavelength range.

Chapter 3. Results and Discussion

3.1. Powder Synthesis

3.1.1 Reaction Equation & Thermodynamic Aspects

For combustion synthesis method, an exothermic reaction will occurs at low temperature that becomes self-sustaining within a short time, resulting in a powder as final product.

Reaction equation as shown below:

$$\begin{aligned} \mathrm{Mg(NO_3)_2} \cdot 6H_2O + 2\mathrm{Al(NO_3)_3} \cdot 9H_2O + 2.222C_6H_8O_7 \\ = MgAl_2O_4 + 13.33CO_2 + 32.89H_2O + 4N_2 \end{aligned} \tag{1}$$

Thermochemical data are taken from references [11, 12]. These data are shown in **Table 3.1**. In **Table 3.1**, "Cp" is a heat capacity, "ΔH_{298K}" is an enthalpy of formation at 298K.

Heat of reaction at 298K for the equation (2) is calculated as ΔH_{298K}=-2267 kJ/mol, and the adiabatic temperature (the maximum temperature reached under adiabatic conditions, with no energy loss)[13] is calculated from the following equation.

$$\Delta_r H^{\circ}_{298} = \int_{298}^{T_{ad}} \sum \left(n_i C_{P_i}\right) dT \tag{2}$$

T_{ad}=1023℃.

However, since the synthesis is not carried out in adiabatic environment, the actually achievable temperature is lower than the calculated value.

Table 3.1 Thermochemical properties of materials related in combustion synthesis of magnesium aluminate spinel

Substances	C_{p298K} [J·mol^{-1}·K^{-1}]	△H_{298} [kJ·mol^{-1}]
CO_2	$51.13+4.37 \cdot T^{-3}-1.47 \cdot 10^{6} \cdot T^{-2}$	-393.51
H_2O	$34.38+7.84 \cdot T^{-3}-0.42 \cdot 10^{6} \cdot T^{-2}$	-241.83
N_2	$30.42+2.51 \cdot T^{-3}-0.24 \cdot 10^{6} \cdot T^{-2}$	0
$MgAl_2O_4$	$146.36+0.04 \cdot T-3.63 \cdot 10^{6} \cdot T^{-2}$	-2299.90
$Mg(NO_3)_2 \cdot 6H_2O$	-	-2613.30
$Al(NO_3)_3 \cdot 9H_2O$	-	-3589.01
$C_6H_8O_7$	-	-1548.80

3.1.2. TGA-DSC

TGA-DSC analysis for the precursors was carried out in order to investigate the combustion reaction. (**Fig. 3-1**) And the XRD patterns of the precursor and the calcined powders at different temperatures are shown in **Fig.3-2**.

According to the XRD results, the precursor is a mixture of NH_4NO_3 and the amorphous matrix. NH_4NO_3 forms from the reaction of nitrates (NO_3^-) and the ammonium cations (NH_4^+).

At about 254℃, DSC graph (**Fig.3-1**) shows a small endothermic peak accounted for 20wt% weight loss in TGA, which is resulted from the dehydration of the precursor.

The first exothermic peak at about 317℃ with a 13wt% weight loss is due to the combustion of ammonium nitrate and citrates.

Since the decomposition temperature of the ammonium nitrate is less than the combustion temperature of citric acid, ammonium nitrate is preferentially decomposed. At the same time, the heat released by the decomposition reaction will result in a partial combustion reaction.

Some of the possible reactions of ammonium nitrate decomposition are listed below[14]

$$NH_4NO_3 \xrightarrow{169℃} N_3O + 2H_3O \tag{3}$$

$$4NH_4NO_3 \xrightarrow{>230℃} 2N_2 + 2N_2O + O_2 + 8H_2O \tag{4}$$

$$5NH_4NO_3 \xrightarrow{300℃} 4N_2 + 2HNO_3 + 9H_2O \tag{5}$$

The second exothermic peak at about 485℃ is caused by the combustion of the remaining fuel.[15] Further heating causes a small exothermic peak at 800℃ without weight loss, according to the XRD pattern, which can be assigned to the crystallization of $MgAl_2O_4$ spinel.

TGA-DSC curves obtained from the precursor added with 1wt% LiF are shown in **Fig.3-3**. According to the result of the XRD patterns from different temperatures (**Fig. 3-4**), the spinel forms when the calcination temperature is higher than 340℃. It can be infer that the spinel formation temperature is reduced from 800℃ to 290℃.

The first exothermic peak is higher and sharper than the control group, which means that the combustion reaction is more intense after introducing LiF additive.

Referring to the previous report, the primary carbonaceous material left in the batch is a source of heat sink, which will slow down the reaction.[16] However, the F^- can react with the C and formed CF_4 gas phase, remove the heat sink (Equation 6 & 7, **Table 3.2 & 3.3**). The Elemental analysis was carried out in order to detect the carbon contamination in the powders (**Fig.3-5**). Through the result, we found that the carbon concentration was significantly reduced by the aid of LiF additive.

$$2F_2 + C \rightarrow CF_4 \quad (6)$$

$$4\mathrm{HF} + \mathrm{C} + O_2 \rightarrow CF_4 + 2H_2O \quad (7)$$

The similar phenomenon was also reported by the other researchers, when the LiF was used as the sintering additive.[17]

But the introduction of the LiF will lead to the formation of impurities. By comparing the XRD patterns before and after 659°C, it is found that the exothermic reaction at 689°C corresponds to the formation of impurities (Equation 8 & 9).

$$Li_2O + MgAl_2O_4 \rightarrow 2LiAlO_2 + MgO \quad (8)$$

$$2LiF + MgAl_2O_4 \rightarrow 2LiAlO_2 + MgF_2 \quad (9)$$

Due to no more weight loose after 800°C. So, we chose 800 900 1000°C as the calcination temperature to synthesis MAS.

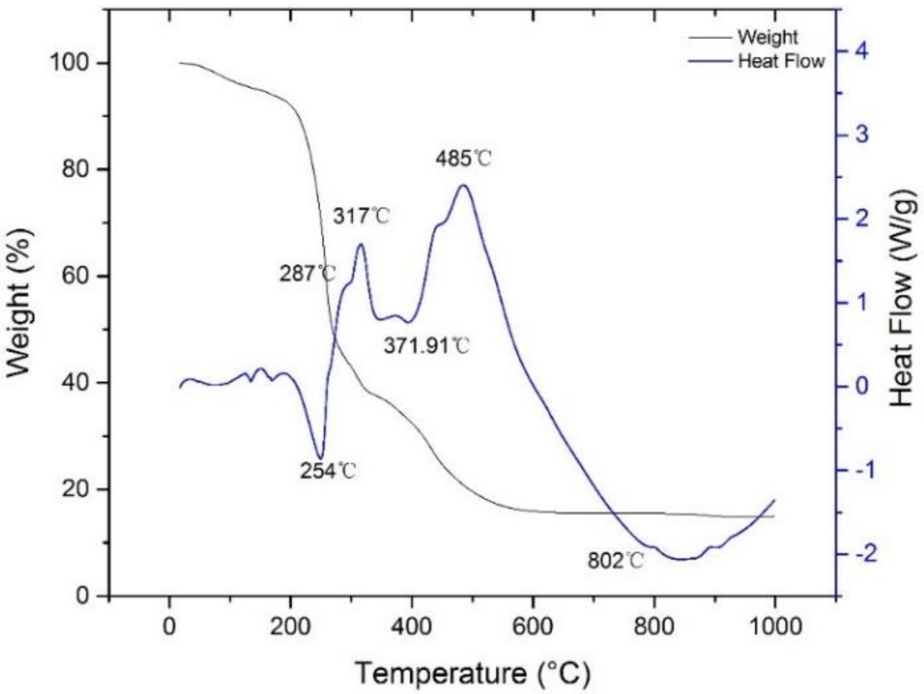

Fig. 3-1 TGA/DSC curves of $MgAl_2O_4$ spinel precursor (without LiF additive).

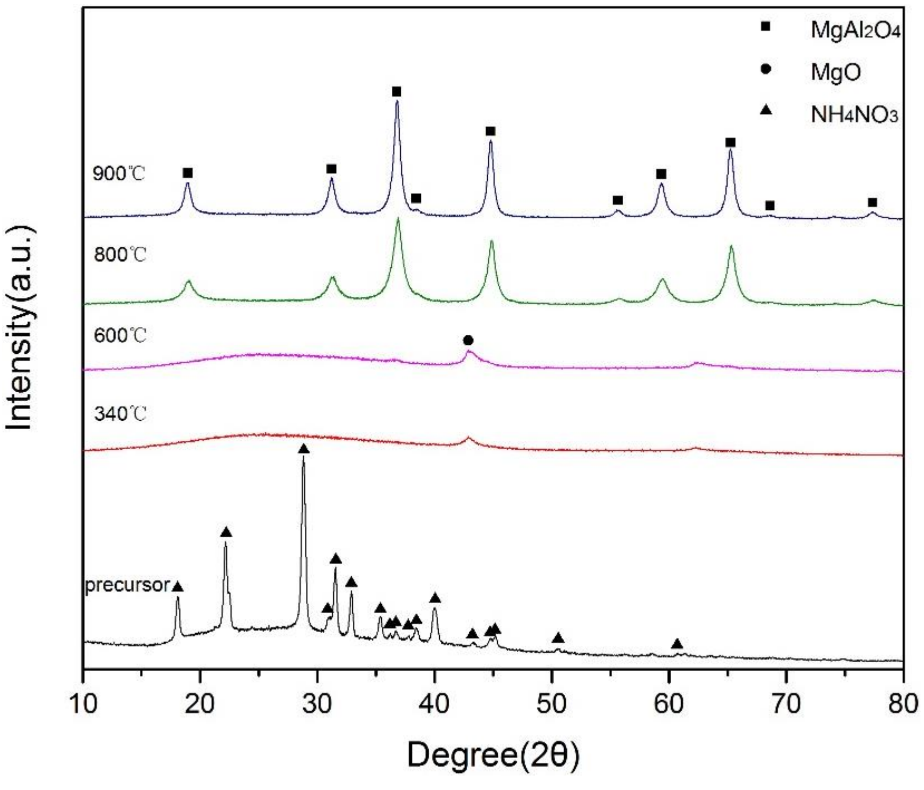

Fig. 3-2 XRD patterns of the dried and calcined precursor at different temperatures (without LiF additive).

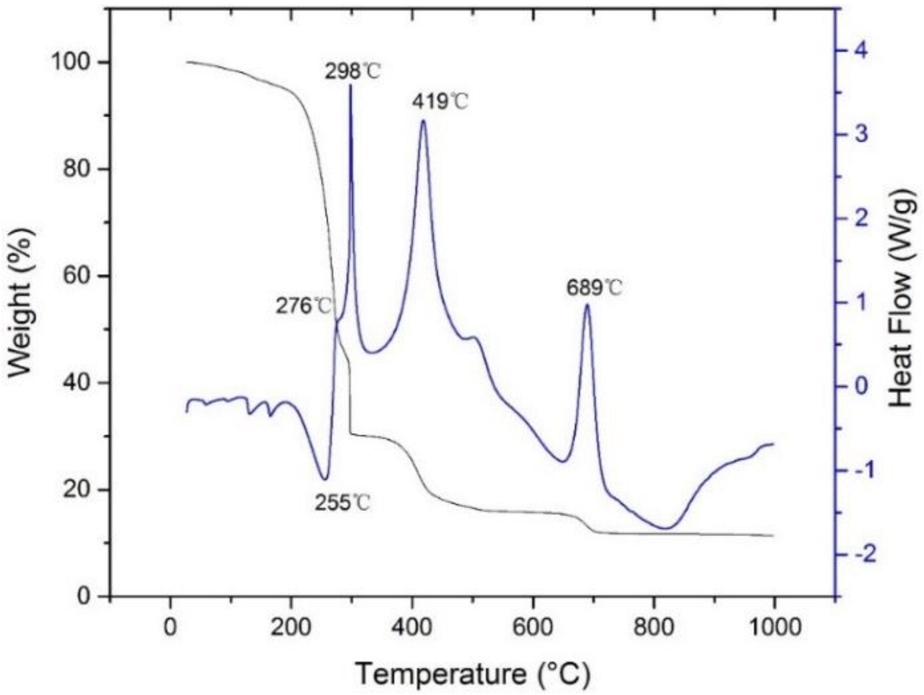

Fig. 3-3 TGA/DSC curves of $MgAl_2O_4$ spinel precursor (with 1wt% LiF additive).

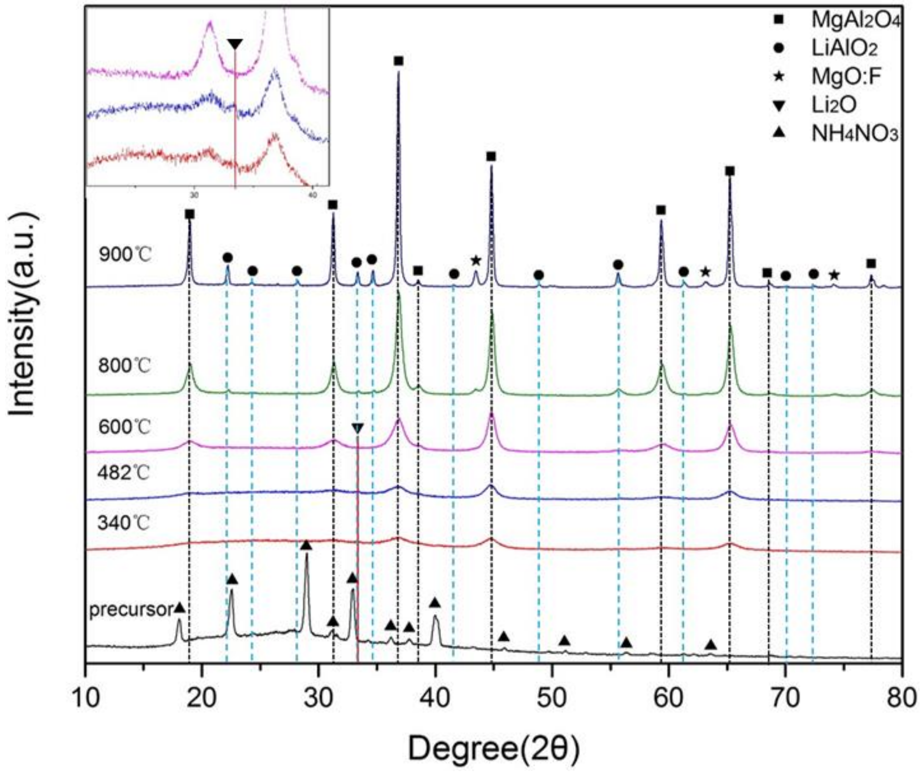

Fig. 3-4 XRD patterns of the dried and calcined precursor at different temperatures (with 1wt% LiF additive).

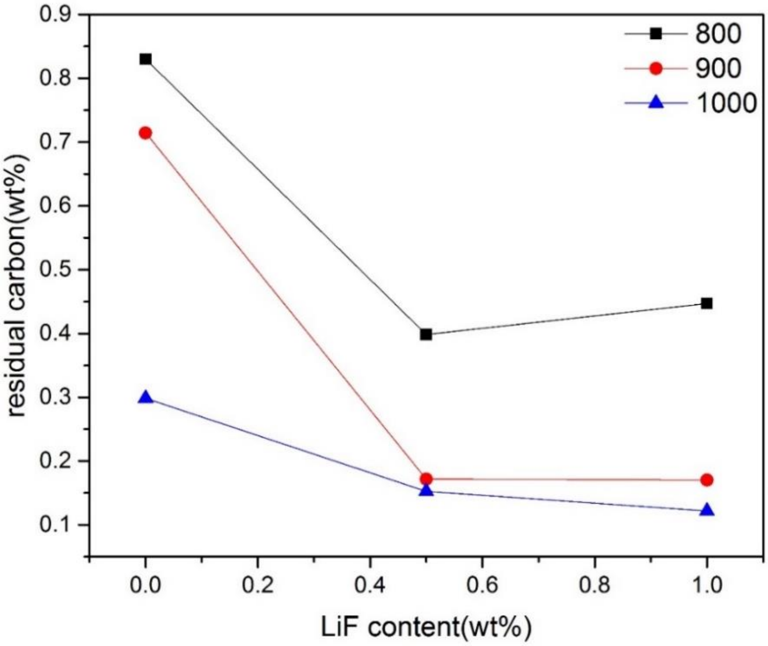

Fig. 3-5 Carbon concentration of the powders synthesized at different temperature with different amounts of LiF(Element Analyzer)

Table 3.2 The change ΔG in Gibbs Free Energy of reaction 6

T(K)	ΔG=ΔH - TΔS
298	-888.5
300	-888.2
400	-873.1
500	-857.8
600	-842.5
700	-827.1
800	-811.8
900	-796.5

Table 3.3 The change ΔG in Gibbs Free Energy of reaction 7

T(K)	ΔG=ΔH - TΔS
298	-247.2
300	-246.7
400	-219.6
500	-192.1
600	-164.4
700	-136.5
800	-108.6
900	-80.8

3.2. Material characterization of as-obtained $MgAl_2O_4$

3.2.1. Particle Morphology

Through the FE-SEM results (**Fig.3-6**), we can see that the introduction of LiF significantly change the particle morphology.

Without the additive, the morphology of powder consists of hard agglomeration of round shaped particles. The average particle size didn't changed a lot with the calcination temperature.

However, with the aid of LiF, the faceted spinel grain appeared due to the liquid phase formation when the calcination temperature was higher than 900°C, taking into account that the melting point of LiF is about 845°C. And also, it has been report that $MgAl_2O_4$ crystallites grown in the melt have octahedral habit, which is an equilibrium form of spinel crystals.[18] Through the FE-SEM result, the octahedrons are mainly faceted by (111) planes.

Meanwhile, the quantity of the highly faceted grain increased with the concentration of LiF.

Through the TEM result (**Fig. 3-7**), it can be seen that the introduction of additive reduces the particle agglomeration degree.

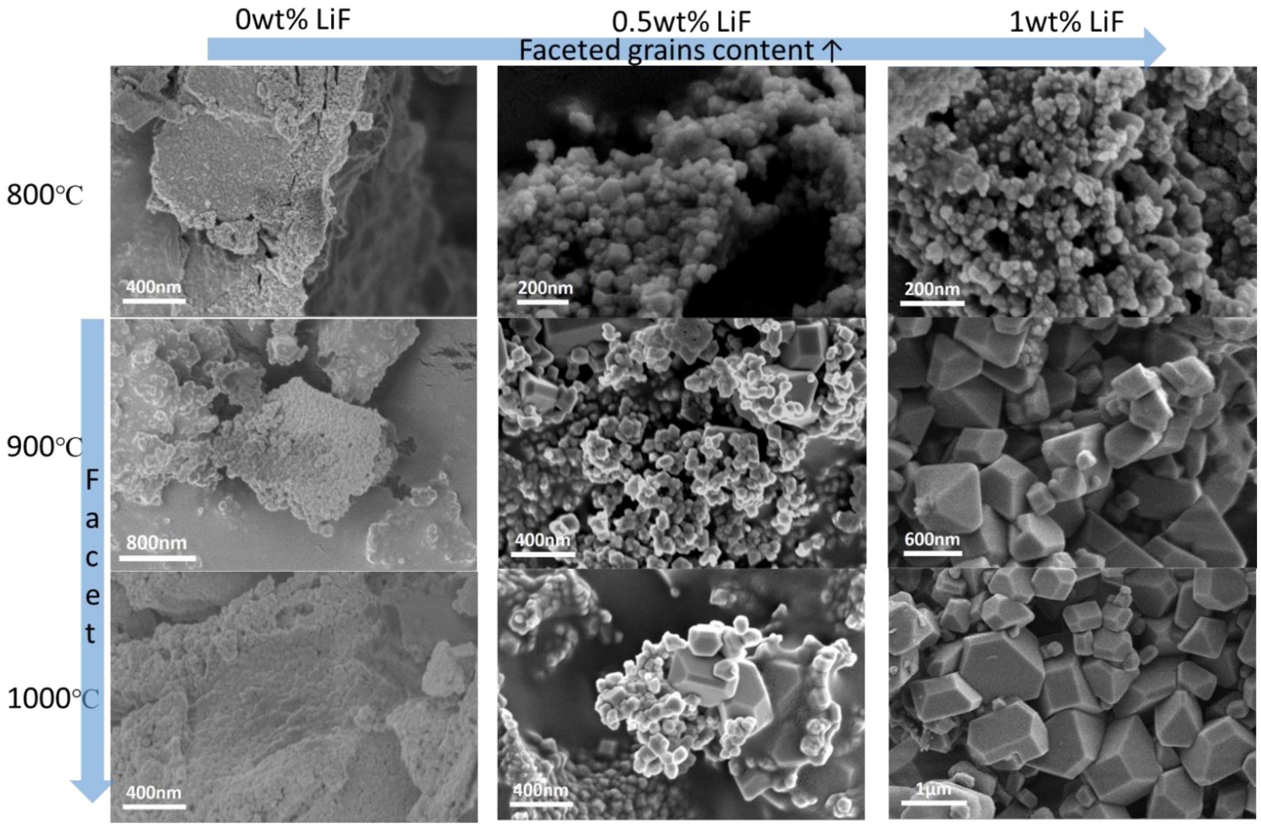

Fig. 3-6 FE-SEM micrograph of $MgAl_2O_4$ prepared by combustion synthesis method with different amount of LiF at different temperature

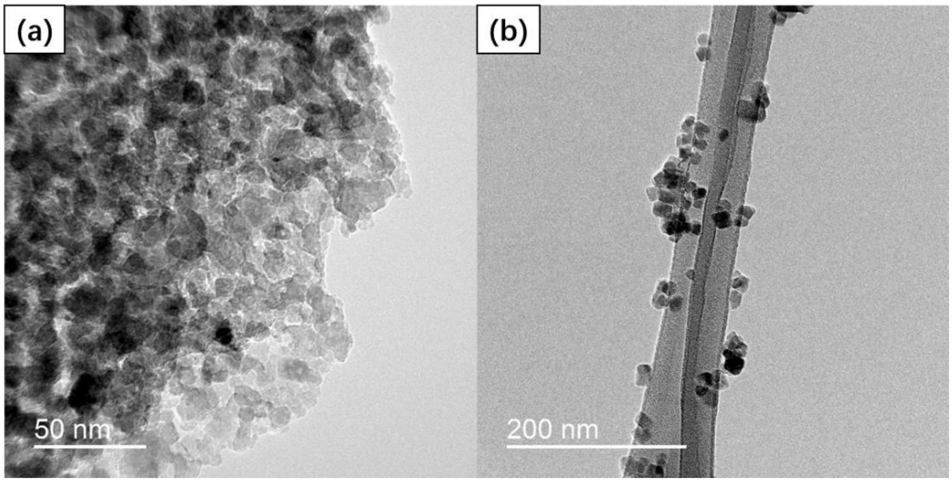

Fig. 3-7 TEM micrograph of $MgAl_2O_4$ prepared at same temperature (800℃-1h) with different amount of LiF (a) 0wt%; (b) 1.0wt%

3.2.2. Different Additives

The experiment was repeated by the different additives LiCl & AlF_3, respectively, in order to find out how the LiF contribute to the combustion synthesis method.

As the typical molten salt additive, the melting temperature of LiCl is ~600℃. For the sample heated at 1000℃ with the LiCl additive, as shown in **Fig.3-8-(c)**, the particles were combined by the soft agglomeration. Some highly-facet grains occurs due to a liquid phase formation. In contrast, the particle size is much smaller than the one synthesized by the LiF additive. The particles size was in range of 55~110 nm with regular shape. It's believed that LiCl can reduce the particle agglomeration degree and doesn't coarsen the particles.

However, for another additive AlF_3, the carrier of F^-, has a melting point of 1040℃ which is higher than the adiabatic temperature (T_{ad}) and the calcination temperature (1000℃). It's difficult to form a liquid phase during the synthesis process. The FE-SEM graph (**Fig.3-8-(d)**) shows that, the introduction of AlF_3 could significantly increase the particle size. But the particles still combined with the hard agglomeration.

Therefore, it can be infer that LiF as molten salt can reduce the agglomeration degree, and the F ion can coarsen the particle size.

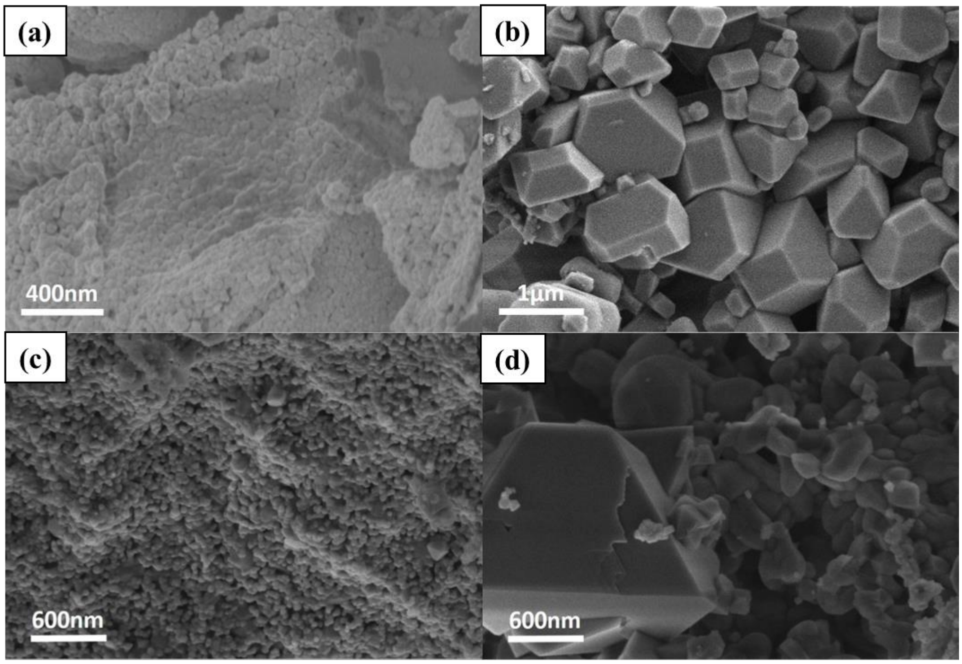

(a) without additive; (b) 1wt% LiF ; (c) 1wt% LiCl; (d) 1wt% AlF_3

3.2.3. Impurity

The XRD pattern at the high calcination temperature indicate that the introduction of LiF also leads to the formation of secondary phases.

And these impurities can be removed through the washing treatment by HCl.

The reactions between impurities and HCl are shown below:

$$\mathrm{LiAlO_2} + 4HCl \rightarrow LiCl + AlCl_3 + 2H_2O \quad (10)$$

$$\mathrm{MgO} + 2\mathrm{HCl} \rightarrow MgCl_2 + H_2O \quad (11)$$

$$MgF_2 + 2\mathrm{HCl} \rightarrow MgCl_2 + 2HF \quad (12)$$

Combine the result of XRD pattern (**Fig.3-9**) and FE-SEM graph (**Fig.3-10**). It can be inferred that the impurity exist in the surface of high crystallinity particles. Without any post-treatment, these impurities will react with each other at 1300°C formed MAS and other gas phase (Equation 13 & 14). [17]

$$\mathrm{Mg}O + 2\mathrm{LiAlO_2} \xrightarrow{1300} MgAl_2O_4 + Li_2\mathrm{O(g)} \quad (13)$$

$$\mathrm{Mg}F_2 + 2\mathrm{LiAlO_2} \xrightarrow{1300} MgAl_2O_4 + 2\mathrm{LiF(g)} \quad (14)$$

The gas phase generated during the sintering process results in the formation of the porous structure as shown in **Fig.3-10**. These pores can be treated as scattering sources that reduce the transparency of the ceramic. Which means the washing process is necessary

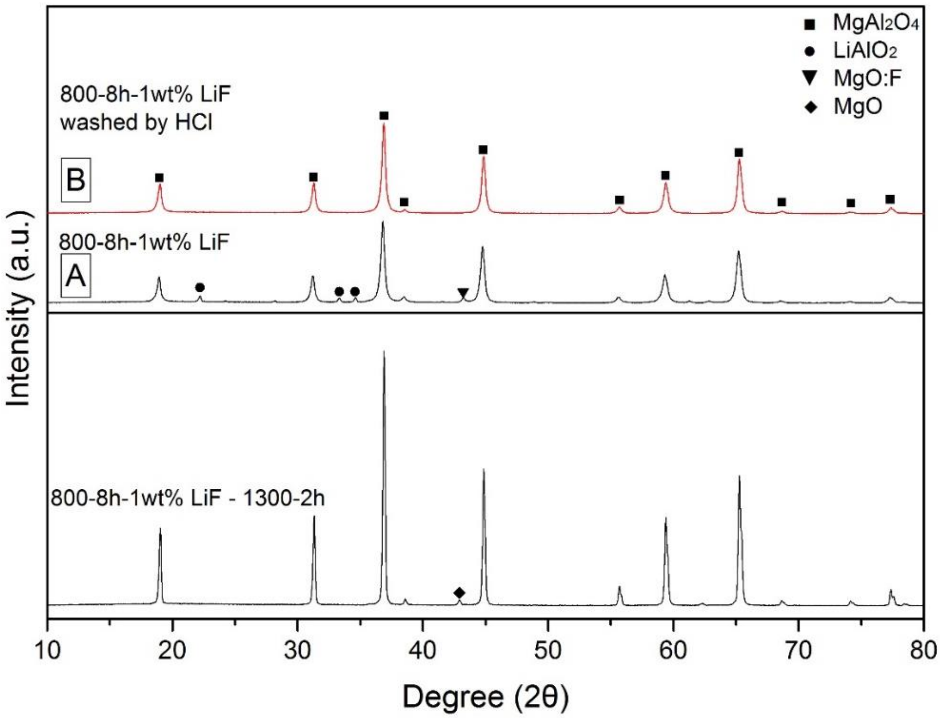

Fig. 3-9 XRD pattern of $MgAl_2O_4$ powder prepared by combustion synthesis at 800°C (A) before and (B) after washing treatment, and by post-calcination at 1300°C with 1wt% LiF additive

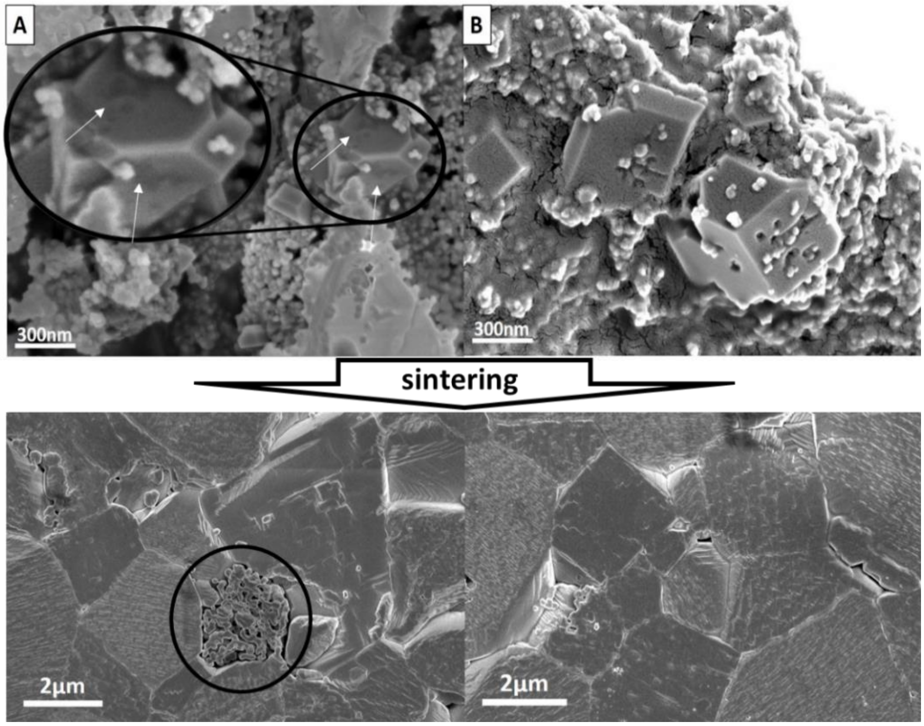

Fig. 3-10 FE-SEM micrograph of $MgAl_2O_4$ prepared by combustion synthesis method with 1wt% LiF additive at 800°C-1h (A) before and (B) after washing treatment. And the surface morphology of sintered samples (1550°C-2h).

3.2.4. 2-steps calcination

However, the size of impurities increased with the calcination temperature. After washing treatment, several holes appear on the surface of the particles, resulting in the irregular shapes of particles. (**Fig.3-11 &Fig.3-12**) This irregularity may lead to the low sinterability of particles.

In order to improve the sinterability, surface regularity is required. So, in this process, 2-steps calcination was carried out at low temperature and relatively high temperature. In the low temperature of 800℃, the particles are prevented from coarsening and the impurities are readily removed by washing treatment. Hence, the particles can retain relatively small average size and low residue carbon concentration after calcined at high temperature of 1000℃. (**Fig.3-13**)

Fig.3-14 illustrates the influence of different amounts of LiF on the morphology of 2-steps calcined $MgAl_2O_4$ powders. Introduction of 0.5wt% LiF, led to a high purity of powder (**Fig.3-14-(a)**) with small particle size and narrow particle size distribution. However as the LiF concentration increased to 1wt%, the powders (**Fig.3-14-(b)**) possess polydisperse particle size distribution having two fractions with particle size of 600-1100nm and ~160nm.

Denoted the powder synthesized by 2-steps calcination with 0.5wt% LiF as '**MgAl-2steps-0.5wt%**', and the powder synthesized with 1.0wt% LiF as '**MgAl-2steps-1.0wt%**'.

The binary mixture of nonspherical particles of different sizes is beneficial for achieving a high packing density during compaction.[5, 19]

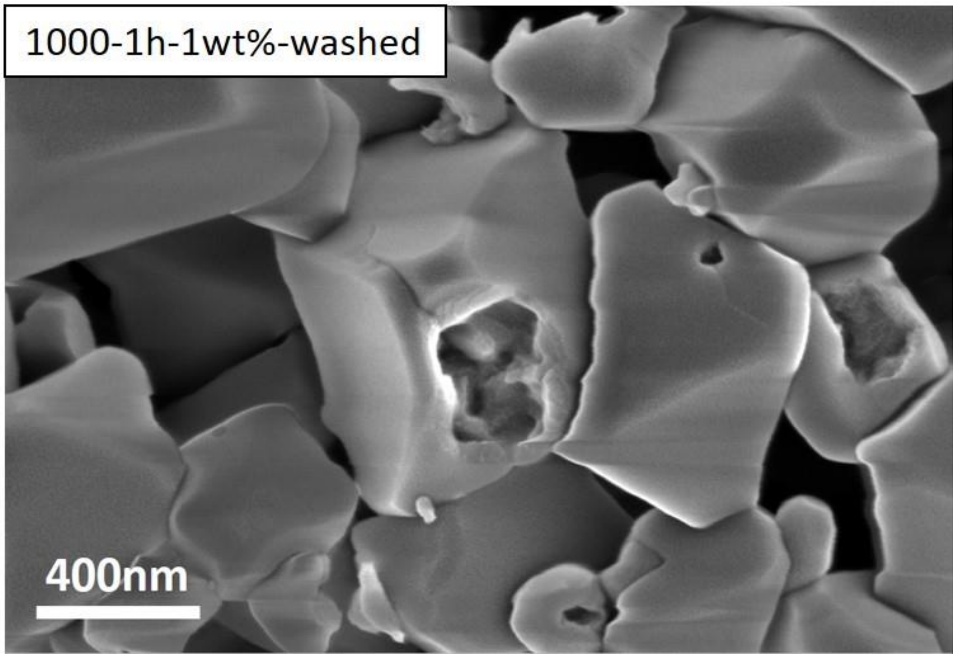

Fig. 3-11 FE-SEM micrograph of $MgAl_2O_4$ prepared by combustion synthesis method at 1000°Cwith 1wt% LiF additive after washing treatment

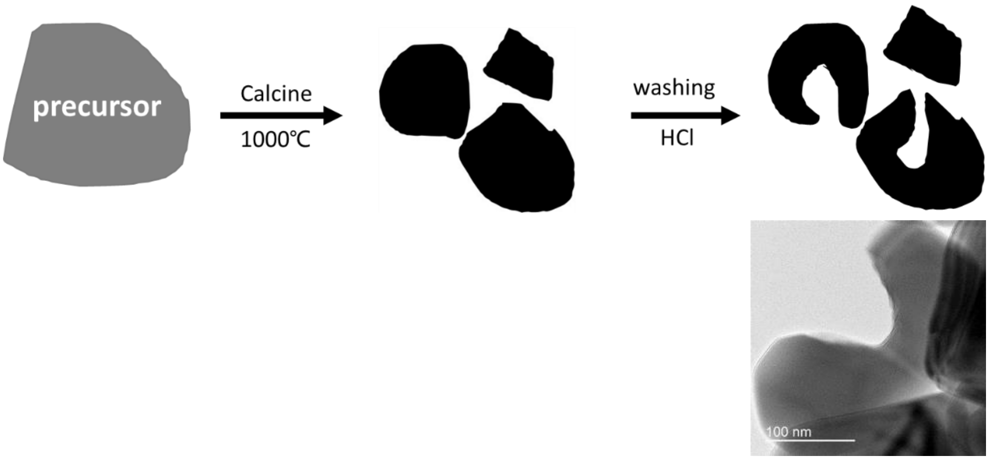

Fig. 3-12 Schematic diagram of the washing treatment and the TEM micrograph of the $MgAl_2O_4$ particle prepared by combustion synthesis method after washing treatment

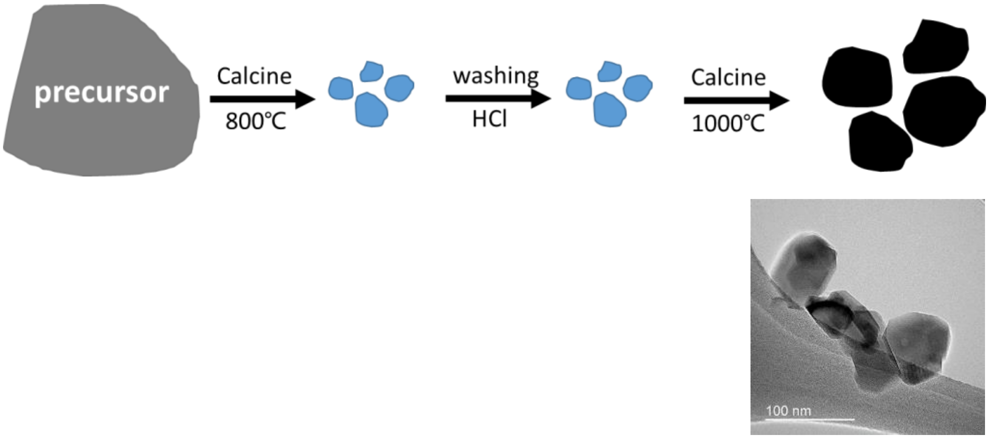

Fig. 3-13 Schematic diagram of the 2-steps calcination and the TEM micrograph of the $MgAl_2O_4$ particle synthesized by 2-steps calcination combustion method after washing treatment

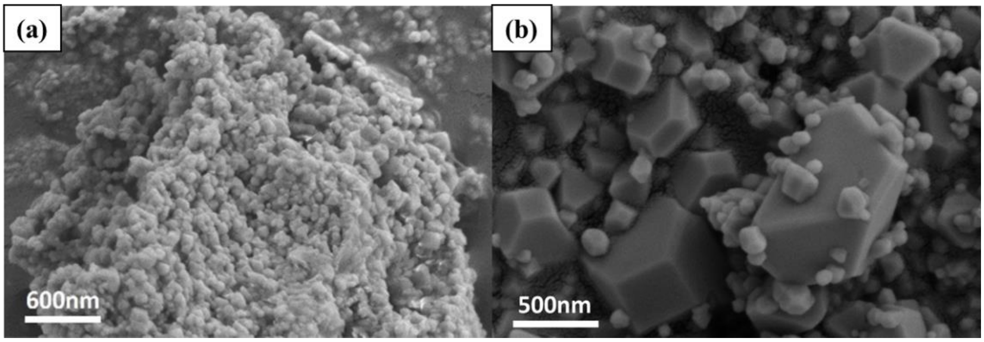

Fig. 3-14 FE-SEM micrograph of $MgAl_2O_4$ prepared by 2-steps calcination combustion synthesis method with (a) 0.5wt% LiF & (b) 1.0wt% LiF additive.

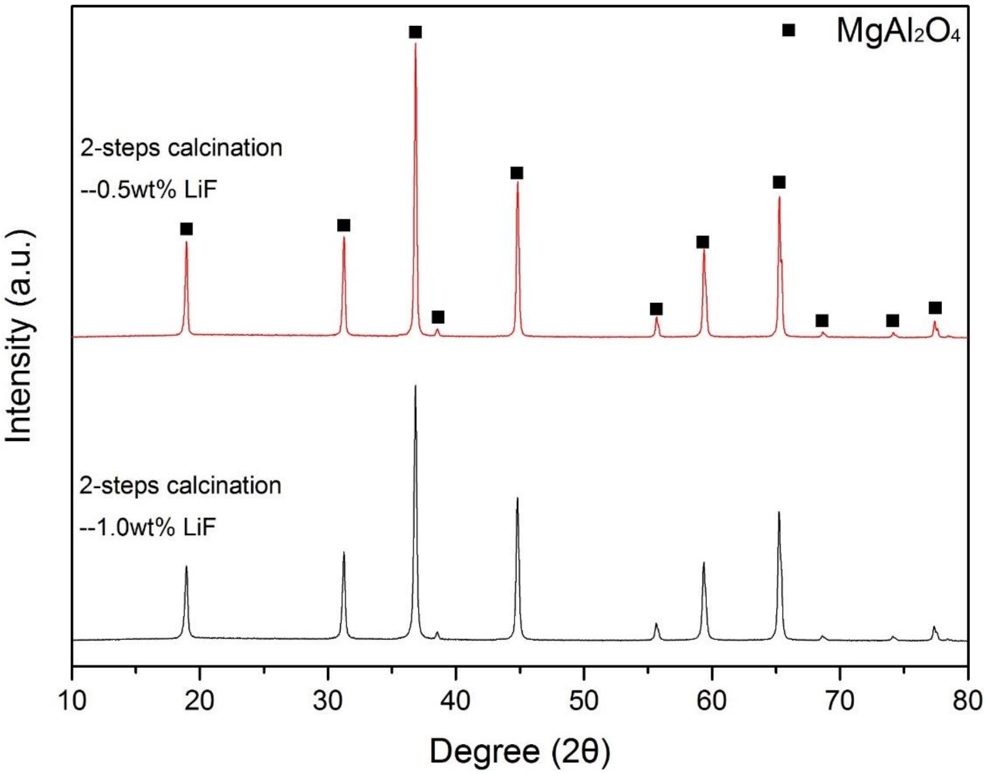

Fig. 3-15 XRD pattern of MgAl2O4 powder prepared by 2-steps calcination combustion synthesis method with different amounts of LiF additive

3.3. Sintering

3.3.1. Air Sintering

The relative density of sintered samples for different calcination temperature and LiF concentration could be seen from **Table 3.4** and **Fig.3-16**. Samples sintered by 2-step calcined powders exhibited higher relative densities, 94.2% and 93.8%, respectively, than samples sintered by 1-step calcined powders. The results indicate that the two-step calcination method can improve the powder sinterability.

It has been reported that transparent spinel is difficult to fabricate directly from high purity precursor powders by using the conventional pressureless sintering techniques.[20-23] In order to obtain a transparent spinel, SPS method was used.

Table 3.4 Relative density of bulk samples sintered at 1550°C for 2h.

No.	Calcin. Temp. (°C)	LiF	Relative density(%)
1	800-1h	0wt%	73.8
2		0.5wt%	82.1
3		1.0wt%	76.2
4	1000-1h	0wt%	64.8
5		0.5wt%	92.5
6		1.0wt%	87.2
7	800-1h-washed 1000-1h	0wt%	73.4
8		0.5wt%	**94.2**
9		1.0wt%	**93.8**

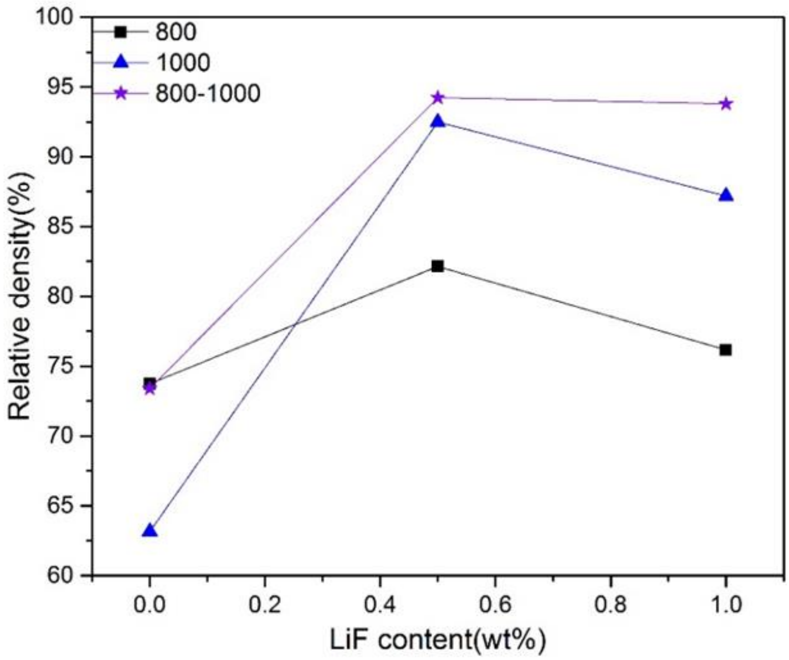

Fig. 3-16 Relative density of bulk samples sintered at 1550°C for 2h.

3.3.2. SPS

Fig.3-17 shows the appearance of the samples SPSed under various sintering temperature. The transparency apparently depends on the sintering temperature.

The powder, **MgAl-2steps-0.5wt%**, show the best performance in transparency when the sintering temperature is 1200℃. However, for the powder **MgAl-2steps-1.0wt%**, the best performance sintering temperature is 1300℃.

The total forward transmission spectrum of the best performance samples for each powders are shown in **Fig.3-18**. The total-forward transmission of 0.3mm thick **MgAl-2steps-0.5wt%** and 1.1mm thick **MgAl-2steps-1.0wt%** transparent ceramics reaches 81% and 75% at the wavelength of 1600nm, respectively.

Further studies are needed to analyze the micromorphology of sintered samples and the optimum sintering condition.

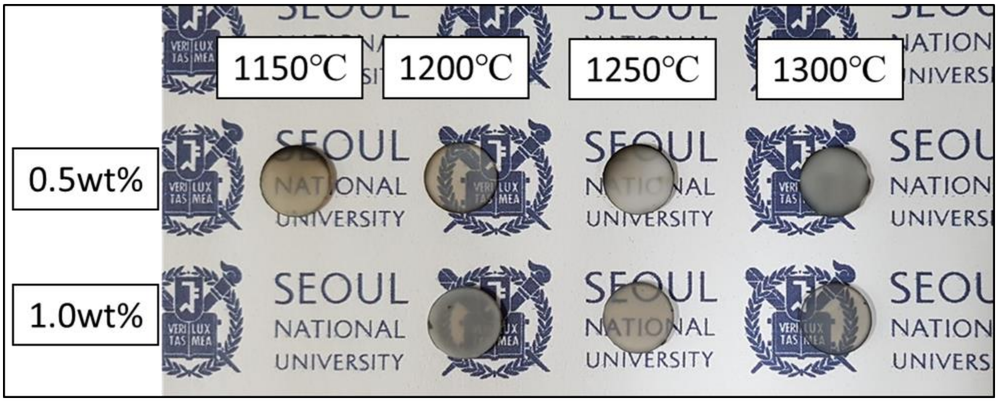

Fig. 3-17 The appearance of the specimens fabricated by SPS with the powder prepared by 2-steps calcination combustion synthesis method.

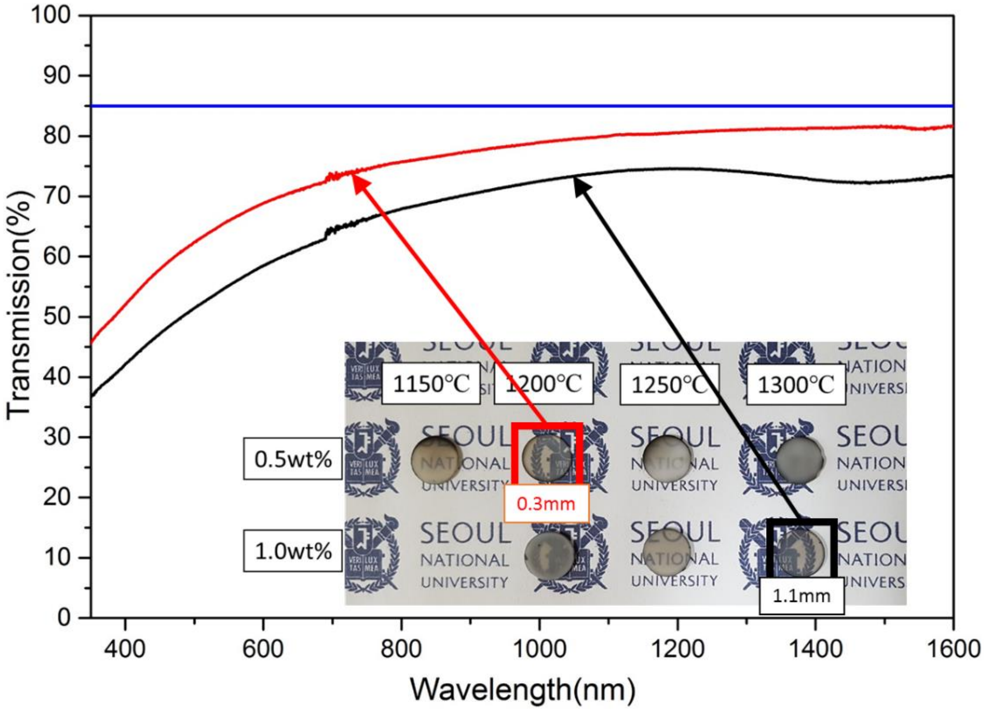

Fig. 3-18 The total-forward-transmission of two, 0.3mm-thick 0.5wt%-1200℃ (red line) and 1.1mm-thick 1.0wt%-1300℃ (black line) spinel specimens as a function of the wave-length.

Chapter 4. Conclusions

In conclusion, combustion synthesis method was improved by the LiF additive and the 2-steps calcination. It has been determined that LiF sintering aid significantly lower the spinel formation temperature from 800℃ to 290℃. As the result, the synthesized powder

1. have the low carbon contamination of about 0.09wt%.
2. have the low agglomeration degree
3. have the good sinterability.
4. have the low sintering temperature of about 1200℃.

Transparent **MgAl-2steps-0.5wt%** ceramic possessing total-forward transmission of 81% at λ=1600nm was obtained by SPS sintering at 1200℃ for 20min holding.

Reference

1. Han, J., et al., *Phosphor development and integration for near-UV LED solid state lighting.* ECS Journal of Solid State Science and Technology, 2013. **2**(2): p. R3138-R3147.
2. Harris, D.C. *History of development of polycrystalline optical spinel in the US*. in *Proc. SPIE*. 2005.
3. Rubat du Merac, M., et al., *Fifty Years of Research and Development Coming to Fruition; Unraveling the Complex Interactions during Processing of Transparent Magnesium Aluminate (MgAl2O4) Spinel.* Journal of the American Ceramic Society, 2013. **96**(11): p. 3341-3365.
4. du Merac, M.R., *The role of impurities, LIF, and processing on the sintering, microstructure, and optical properties of transparent polycrystalline magnesium aluminate (MgAl 2 O 4) spinel*. 2014: Colorado School of Mines.
5. Balabanov, S.S., et al., *Fabrication of transparent MgAl2O4 ceramics by hot-pressing of sol-gel-derived nanopowders.* Ceramics International, 2015. **41**(10): p. 13366-13371.
6. Meir, S., et al., *Synthesis and Densification of Transparent Magnesium Aluminate Spinel by SPS Processing.* Journal of the American Ceramic Society, 2009. **92**(2): p. 358-364.
7. Rozenburg, K., et al., *Sintering Kinetics of a MgAl2O4Spinel Doped with LiF.* Journal of the American Ceramic Society, 2008. **91**(2): p. 444-450.
8. Jiao, H., et al., *Low temperature synthesis of YAG:Ce phosphors by LiF assisted sol–gel combustion method.* Powder Technology, 2010. **198**(2): p. 229-232.
9. Kostić, E., S. Bošković, and Š. Kiš, *Influence of fluorine ion on the spinel synthesis.* Journal of Materials Science Letters, 1982. **1**(12): p. 507-510.
10. Morita, K., et al., *Effect of loading schedule on densification of MgAl2O4 spinel during spark plasma sintering (SPS) processing.* Journal of the European Ceramic Society, 2012. **32**(10): p. 2303-2309.
11. Barin, I., *Thermochemical Data of Pure Substances, Thermochemical Data of Pure Substances*. 1997: Wiley-VCH.
12. Speight, J.G., *Lange's handbook of chemistry*. Vol. 1. 2005: McGraw-Hill New York.
13. Ianos, R., et al., *Solution combustion synthesis of strontium aluminate,*

SrAl2O4, powders: single-fuel versus fuel-mixture approach. Phys Chem Chem Phys, 2016. **18**(2): p. 1150-7.

14. Saberi, A., et al., *Chemical synthesis of nanocrystalline magnesium aluminate spinel via nitrate–citrate combustion route.* Journal of Alloys and Compounds, 2008. **462**(1-2): p. 142-146.
15. Saberi, A., et al., *A novel approach to synthesis of nanosize MgAl2O4 spinel powder through sol–gel citrate technique and subsequent heat treatment.* Ceramics International, 2009. **35**(3): p. 933-937.
16. Saberi, A., et al., *A novel approach to synthesis of nanosize MgAl 2 O 4 spinel powder through sol–gel citrate technique and subsequent heat treatment.* Ceramics International, 2009. **35**(3): p. 933-937.
17. Rozenburg, K., et al., *Chemical Interaction Between LiF and MgAl2O4Spinel During Sintering.* Journal of the American Ceramic Society, 2007. **90**(7): p. 2038-2042.
18. Dekkers, R. and C. Woensdregt, *Crystal structural control on surface topology and crystal morphology of normal spinel (MgAl 2 O 4).* Journal of crystal growth, 2002. **236**(1): p. 441-454.
19. Kong, L.B., et al., *Transparent Ceramic Materials*, in *Transparent Ceramics*. 2015, Springer. p. 29-91.
20. Wang, S.F., et al., *Transparent ceramics: Processing, materials and applications.* Progress in Solid State Chemistry, 2013. **41**(1-2): p. 20-54.
21. Dericioglu, A. and Y. Kagawa, *Effect of grain boundary microcracking on the light transmittance of sintered transparent MgAl 2 O 4.* Journal of the European Ceramic Society, 2003. **23**(6): p. 951-959.
22. Bratton, R., *Translucent sintered MgAl2O4.* Journal of the American Ceramic Society, 1974. **57**(7): p. 283-286.
23. Li, J.G., et al., *Fabrication of translucent magnesium aluminum spinel ceramics.* Journal of the American Ceramic Society, 2000. **83**(11): p. 2866-2868.

국문 초록

김 건 (Jin Jian)

재료공학부

대학원

서울대학교

우수한 기계적 특성과 near-UV에서 mid-IR (190 $<\lambda<$6000nm)까지의 높은 투명성으로 인해 $MgAl_2O_4$는 방탄 창 시스템, 고 에너지 레이저 창 및 경량의 갑옷과 같은 광학 공학 응용 분야에 사용되었다.

고품질의 투명 세라믹을 제조하기 위해서 고품질의 시작 분말이 필요한다.

그래서 우리는 최근 여러 가지 장점으로 인해 연구자들의주의를 끄는 연소 합성 방법을 사용했다. 그러나 연소 합성 방법은 아직 몇 가지 단점을 극복해야한다. 스피넬 형성 메커니즘을 통해 첨가제를 도입하기로 결정했다. 계산 후, LiF 첨가물의 가능성이 인증되었다.

LiF의 함량 변화에 따라 합성 조건, 분말 특성, 열역학적 측면 및 소결성과 관련하여 $MgAl_2O_4$ (MAS)의 연소 합성이 연구되었다.단일 연료로 시트르산을 사용하면 투명한 세라믹 원료로 사용할 수없는 높은 탄소 오염과 빈약 한 소결성을 가진 MAS 만 얻을 수있다. 그러나, LiF를 도입함으로써, 양호한 특성의 MAS 분말을 합성 할 수있다. 이는 LiF가 효과적으로 MAS의 형성 에너지를 감소시키고, 잔류 탄소를 제거하고, 응집도를 감소시키고 연소 반응 동안 결정 성장을 촉진시킬 수 있기 때문이다. 2 단계 가열과정을 통해 얻었던 고순도 분말은 T=1200℃, P = 80MPa에서 20 분 동안holding SPS에 의해 투명 세라믹 (T = 81.0 %)으로 소결되었다

핵심어: $MgAl_2O_4$, Nanocrystals, Combustion synthesis, LiF, transparency

학 번: 2015-22306